

Optimised Sensor Selection for Control and Fault Tolerance: comparison and some new results

Konstantinos Michail¹, Argyrios Zolotas² and Roger Goodall³

Abstract—Optimised sensor selection for control design is a non-trivial task to perform especially if the selection is done with respect to complex control requirements like reliability, optimised performance, robustness and fault tolerance. In this paper, a proposed framework is presented aiming to tackle the aforementioned problem. In this context, a Linear Quadratic Gaussian (LQG) controller is presented and applied to an Electro-Magnetic Suspension (EMS) system. Furthermore, the LQG solution is compared to a Multi-Objective ($\mathcal{M.O.}$) \mathcal{H}_∞ and \mathcal{H}_∞ controller design via loop-shaping method using realistic simulations. A particular contribution is the use of Sensor Fault Accommodation Ratio (SFAR) in the LQG scheme providing useful conclusions on the optimised sensor selection for the EMS system. It is concluded that the framework can be extended to other industrial applications.

I. INTRODUCTION

An optimised sensor selection framework under different Modern Control Methods (MCM) is presented. The problem of optimised sensor selection with respect to optimised and robust performance, sensor fault tolerance with the minimum number of sensors and minimum control system complexity is a hard task to do in control system design. In particular, when a number of sensors exist, usually for a particular application under consideration, the question posed is given as: *what is the best sensor set that could be used in order to ensure the required properties of a control system?*. A number of studies on the input/output selection has been done the last years [1] but non of them considers both control and reliability properties of a control system. This attempt is done by the authors with the aim of a systematic framework that is described in this paper. The aforementioned question can be answered using the proposed framework which combines fields from MCM, multiobjective optimisation and Fault Tolerant Control (FTC) provided that the model of the plant is known, to an extend. The proposed systematic framework combines MCM [2], FTC [3] and multiobjective optimisation [4]. The Multiobjective optimisation is based on heuristic methods that have been extensively used in engineering optimisation [5]. Particularly, the Genetic Algorithms (GA) [6] which have been extensively used in control systems [7] are successfully merged into the framework. There are different types of GAs that can be used for addressing

the multiobjective constrained optimisation nature of the problem but in this paper, the Non-dominated Sorting of Genetic Algorithm II (NSGAI) in [8] in combination with penalty functions to handle the control constraints [9] is employed. It is shown that using the proposed framework is possible to offer a level of simplicity in the sensor selection process. A general diagram of the framework is illustrated in Fig.1. The proposed framework has been tested

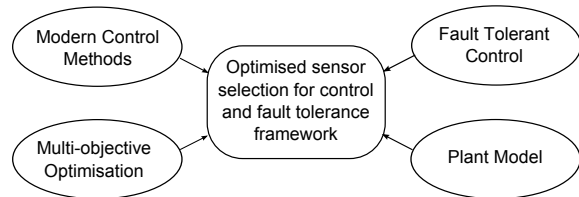


Fig. 1. Schematic of the proposed optimised sensor selection framework.

under various MCM including Linear Quadratic Gaussian (LQG) control [10], Multi-Objective ($\mathcal{M.O.}$) \mathcal{H}_∞ robust control [11] and the \mathcal{H}_∞ Loop-Shaping Design Procedure (LSDP) [12]. A detailed comparison of the results is done in the paper, illustrating issues of simplification and flexibility in the framework. However, required computational power can be a drawback, this being based on how complex the constraints, system and control design may be. The EMS is used for testing purposes of the framework. It is a rather simple nonlinear system, but is inherently unstable and with a set of non-trivial requirements to achieve [13].

This paper is organised as follows: Section II gives a general description of the framework, Section III describes the EMS model, Section IV describes the modern control methods combined with the framework. In Section V the simulation results are presented and the efficacy of the proposed framework is assessed. The paper concludes by summarizing the advantages in Section VI.

II. THE GENERALISED FRAMEWORK

The generalised flowchart of the framework is given in Fig. 2. The particular points include the use of MCM and the heuristic multiobjective optimisation using GAs, with the optimization performed for every feasible sensor set. Prior to running the algorithm (initialization phase), some parameters are assigned including the GA parameters, control objective functions ϕ_i and controller selection criteria (f_{c_i}) and (f_k). f_{c_i} and f_k ensure that the selected controller, k_o , results in a desired closed-loop requirements. Starting the optimisation procedure, the first sensor set is selected and the

¹K. Michail is with Department of Mechanical Engineering and Materials Science and Engineering, Cyprus University of Technology, Limassol, Cyprus. kon_michael@ieee.org

²A. Zolotas is with School of Engineering and Informatics, University of Sussex, United Kingdom. a.zolotas@sussex.ac.uk

³R. Goodall is with Control Systems Group, School of Electronic, Electrical and Systems Engineering, Loughborough University, United Kingdom. r.m.goodall@lboro.ac.uk

evolutionary algorithm seeks the Pareto-optimality between the objective functions ϕ_i subject to control constraints. In the sequence, the algorithm seeks to find the optimised controller by using the overall constraint violation function, Ω and f_{c_i} and f_k . Ω is the sum of the constraint violations which is well described in [11].

$$\Omega(k^{(m)}, f^{(p)}) = \sum_{m=1}^M \omega_m(k^{(m)}) + \sum_{p=1}^P \psi_p(f^{(p)}) \quad (1)$$

where, ω_m is the m^{th} soft constraint violation for the corresponding m^{th} quantity to be constrained, k , and M is the total number of soft constraints. Similarly, ψ is the hard constraint violation for the p^{th} quantity to be constrained, f . Next, the SFAR is evaluated if for the corresponding sensor set there is no constraint violation i.e. $\Omega = 0$. The SFAR is given as

$$SFAR \cong \frac{N_{Y_{o_h}}}{N_{Y_{o_f}}} 100(\%) \quad (2)$$

where Y_{o_h} and Y_{o_f} are the healthy and faulty sensor sets respectively and $N_{Y_{o_h}}$ and $N_{Y_{o_f}}$ are the number of sensor sets in Y_{o_h} and Y_{o_f} respectively. The particular sensor set with the corresponding controller, k_o provides optimised nominal performance under certain fault tolerance. These are saved together with other useful data about the response of the system and the algorithm moves to the next feasible sensor set. The optimisation algorithm iterates until all feasible sensor sets are optimised and finally the optimised sensor set selection is done using the data from the report.

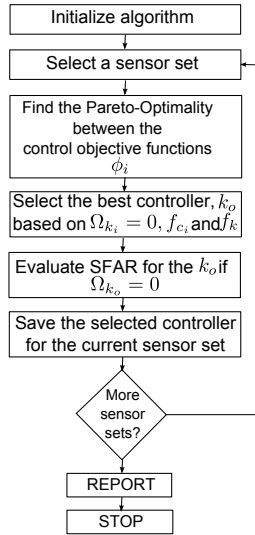


Fig. 2. General algorithm flowchart of the proposed framework.

III. THE EMS SYSTEM

A. Modelling

The single-stage EMS system model represents one quarter of a typical MAGLEV vehicle and is seen as a useful case study to demonstrating the proposed framework. For details

on the particular modelling exercise, the reader is referred to [14]. The non-linear model of the EMS and is given as

$$\frac{dI}{dt} = \frac{V_c - IR_c + \frac{N_c A_p K_b}{G^2} \left(\frac{dz_t}{dt} - \frac{dZ}{dt} \right)}{\frac{N_c A_p K_b}{G} + L_c} \quad (3)$$

$$\frac{d^2 Z}{d^2 t} = g - \frac{K_f}{M_s} \frac{I^2}{G^2}, B = K_b \frac{I}{G} \quad (4)$$

$$F = K_f B^2, \frac{dG}{dt} = \frac{dz_t}{dt} - \frac{dZ}{dt} \quad (5)$$

where V_c is the coil's voltage, F the vertical force, I the coil's current, B , the flux density, M_s the total carriage mass, G the airgap, Z the electromagnet's and z_t the track's position. Constants K_b , K_f and g are the flux, force and gravity constants with values equal to 0.0015, 0.0221 and $9.81m/s^2$ respectively. R_c is the Coil's Resistance, L_c Coil's inductance, N_c Number of turns and A_p Pole face area. The linearisation of the non-linear model is based on small perturbations around the operating point. i.e. the airgap is taken as $G = G_o + (z_t - z)$ with lower case letter defining the small variation around the operating point and subscript 'o' referring to the operating point. Similar approach is done for B , F , I , V_c and Z . The linearized state space description of the EMS is given in (6) with states $x = [i \quad \dot{z} \quad (z_t - z)]^T$ and output equation corresponding to the following five measurements: i the coil's current, b the flux density, $(z_t - z)$ the airgap, \dot{z} the vertical velocity and \ddot{z} the vertical acceleration. Given a total carriage mass of $M_s = 1000kg$, the practical operating point values for the EMS system are $G_o = 0.015m$, $B_o = 1T$, $I_o = 10A$, $V_o = 100V$ and $F_o = 9810N$. Based on the operating point that the EMS should operate, the parameters of the electromagnets can be calculated as: $R_c = 10\Omega$, $L_c = 0.1H$, $N_c = 2000$ and $A_p = 0.01m^2$. Details on suspension's electromagnet design are given in [15].

$$\dot{x} = Ax + B_{u_c} u_c + B_{z_t} \dot{z}_t \quad (6)$$

$$y = Cx$$

B. Disturbance Inputs and Control Requirements

Stochastic Inputs: These are random variations of the rail position as the vehicle moves along the track. Considering the vertical direction, the velocity variations (\dot{z}_t) can be approximated by a double-sided power spectrum density (PSD) and the corresponding autocorrelation function assuming a vehicle velocity, V_v of $15m/s$ and track roughness, $A_r = 1 \times 10^{-7}$ [14].

Deterministic Input: The main deterministic input to the suspension in the vertical direction is due to the transition onto a gradient. In this work, the deterministic input is a rail gradient of 5% at a vehicle speed of $15m/s$, an acceleration of $0.5m/s^2$ and a jerk of $1m/s^3$ [14].

EMS Control Properties: The design requirements for an EMS system depend on the type and operating velocity of the train [16]. The EMS system should support the payload while reject the stochastic inputs (from track roughness)

and follow the deterministic ones (track gradients. Fundamentally, there is a trade-off between the deterministic and stochastic features and there are some limitations that they are allowed to operate tabulated in Table I. The optimised

TABLE I

CONTROL CONSTRAINTS FOR THE ELECTRO-MAGNETIC SUSPENSION.

	Response requirements	Value
Stochastic	RMS acceleration, \ddot{z}_{rms}	$\leq 0.5ms^{-2}$
Track	RMS airgap variation, $(z_t - z)_{rms}$	$\leq 5mm$
Profile	RMS control effort, $u_{c,rms}$	$\leq 300V$
Deterministic	Maximum airgap deviation, $(z_t - z)_p$	$\leq 7.5mm$
Track	Maximum control effort, u_{cp}	$\leq 300V$
Profile	Settling time, t_s	$\leq 3s$
	Airgap steady state error, $e_{(z_t - z)_{ss}}$	$= 0$

TABLE II

CONTROL OBJECTIVE FUNCTIONS FOR EACH CONTROL METHOD.

ϕ_i	LQG		$\mathcal{M.O.} \mathcal{H}_\infty$	\mathcal{H}_∞ LSDP
	LQR	KBE		
ϕ_1	i_{rms}	$\int_0^t x_o - x_a dt$	i_{rms}	i_{rms}
ϕ_2	\ddot{z}_{rms}	$RMS(x_o - x_a)$	γ	γ
ϕ_3	-	$u_{n,rms}$	\ddot{z}_{rms}	\ddot{z}_{rms}
ϕ_4	-	-	$u_{n,rms}$	$u_{n,rms}$

sensor selection problem of the EMS is defined as the best sensor set selection subject to optimised performance and sensor fault tolerance. Particularly, the objective functions to be minimized and control constraints listed on Table II and Table I (for each of the control methods described in Section IV while ensuring performance under sensor faults. The sensor sets can be obtained by using the corresponding rows of the output matrix, C . The total number of sensor sets, N_s is given based on the number of sensors n_s as $N_s = 2^{n_s} - 1$.

IV. MCM AND FTC IN THE CONTEXT OF OPTIMISED SENSOR SELECTION FRAMEWORK APPLIED TO THE EMS

A brief encounter of MCM and the sensor FTC in the context of the proposed framework for optimised sensor selection is given here while rigorous description can be found in [10], [11] and [12].

A. Modern control methods

1) *Multiobjective LQG Control for the EMS*: The LQG controller design is done according to the separation principle, as given in [2]. Only a brief description is included here, while for more details the reader is referred by [10]. The design is done in two steps: (i) The state feedback gains (LQR design), $-K_{lqr}$, are designed and appropriately selected in order to achieve the desirable control properties while the **Kalman-Bucy Estimator (KBE)** is merged into the loop at the second step, in order to provide appropriate state estimation. The LQG control problem is to find the a control u which minimizes the performance index in (7) considering

output regulation. This index has to be calculated for every feasible sensor set used to control the EMS system.

$$J = E \left\{ \lim_{T \rightarrow \infty} \int_0^T [y^T Q y + u^T R u] dt \right\} \quad (7)$$

LQR control for the suspension: The state feedback vector is selected as $x = [i, \dot{z}, (z_t - z), \int z_t - z]^T$ which includes an extra state, the integral action on airgap forming a Proportional plus Integral (P+I) state regulator. The response of this stage is used as reference (or ‘ideal’) for the next stage.

The Kalman-Bucy Estimator design: The linear time-invariant KBE has a state space form formally written as

$$\dot{\hat{x}} = A\hat{x} + B_{u_c}u_c + K_{lqq}(y - C\hat{x}), \quad \hat{y} = C\hat{x} \quad (8)$$

where K_{lqq} is the observer gain matrix that minimizes $E\{[x - \hat{x}]^T[x - \hat{x}]\}$. Minimization can be achieved by appropriately tuning the measurement noise covariance matrix V , and process noise covariance matrix W . During the execution of the framework, the errors between the estimated and the ‘ideal’ states are minimized i.e. the comparison between the closed-loop response with the LQR and the response with the KBE in the loop. The minimization of the errors is performed by the NSGA-II for each sensor set. Therefore the objective functions to be minimized are: (i) the Integral Absolute Error (IAE) for the closed-loop response with deterministic disturbance and (ii) the Root Mean Square Error (RMSE) for the stochastic closed-loop response both given on Table II. An extra objective function is also added which is the RMS value of the noise that appears on the u_c caused from the sensor noise. This makes a total of 7 individual objective functions, where x_o is the vector of the monitored states of interest of the closed-loop with the LQR state feedback (i.e. ‘ideal’ closed-loop response) and x_a are the monitored states of interest of the closed-loop with the KBE, e.g. actual closed-loop (prior to adding sensor noise). After the optimised tuning of the LQG controller for each sensor set, there is a large number of controllers. Hence the Ω in (1), is used to assist with the best controller selection as explained in Section II. However, for a given sensor set there could be many controllers that satisfy the constraints and thus another criterion is needed to make the selection of the best controller. In this context, the following criterion is introduced (given as the sum of the aforementioned objective functions noting the error for deterministic and stochastic responses with and without the KBE)

$$S_f = \sum_{i=1}^{n_x} \phi_{d_i} + \sum_{j=1}^{n_x} \phi_{s_j} \quad (9)$$

where ϕ_{d_i} and ϕ_{s_j} are the objective functions for deterministic and stochastic responses (Three objective functions for each of the responses). n_x is the number of estimated states ($n_x = 3$). In that way it is ensured that the selected controller for the corresponding sensor set satisfies the control constraints and the state estimation is as accurate as possible.

2) $\mathcal{M.O.H}_\infty$ Robust Control for the EMS: The $\mathcal{M.O.H}_\infty$ Robust control design is well documented in the control literature, i.e. see [2]. The aim is to design a controller with which the disturbances mentioned in Section III-B are sufficiently rejected. The problem setup in the context of sensor optimisation is described in [11] where the state space model of the EMS system in (6) is transformed into the following generalised form

$$\begin{aligned} \dot{x} &= Ax + Bz_t w + B_u u_c \\ z_\infty &= C_\infty x + D_{\infty 1} w + D_{\infty 2} u_c \\ y &= C_y x + D_{y1} w + D_{y2} u_c \end{aligned} \quad (10)$$

where w are the exogenous inputs (z_t for the EMS), u_c is the EMS input, z_∞ is the regulated outputs (i.e., u_c the control effort and $(z_t - z)$ the airgap) and y is the corresponding sensor set. Each sensor set is selected by manipulating the output matrix (C_y). The controller is designed in such a way that the infinity norm of the closed-loop transfer function from the exogenous inputs to the regulated outputs is minimised subject to the EMS control requirements mentioned in Section III-B i.e. $\|T_{z_\infty w}\|_\infty < \gamma_{opt}$.

It is worth noting that the controller is stabilizing, thus if necessary another check of controller stability itself might be added. Unstable controllers are not favourable in switching schemes therefore the algorithm rejects all unstable stabilizing controllers. For each sensor set $\|T_{z_\infty w}\|_\infty < \gamma_{opt}$ is solved in MATLAB for each random pair of weighting functions that are produced by the GA using linear matrix inequalities. The weights W_p and W_{u_c} are appropriately selected low and high pass filters (11) to adjust the performance of the controller with parameters tuned using NSGAI. There is no generic procedure to select weighting filters usually being application dependent but some guidelines are given in [2].

$$W_p = \left(\frac{s}{M_p^{1/n_p} + \omega_b} + \omega_b \right)^{n_p} \quad W_{u_c} = \left(\frac{\tau s + A_u^{1/n_u}}{M_u^{1/n_u} s + 1} \right)^{n_u} \quad (11)$$

In the performance weighting (W_p), M_p is the high frequency gain, A_p the low frequency gain and ω_b the crossover frequency. For the control effort weight (W_{u_c}), τ determines the crossover frequency, A_u is the low frequency gain and M_u is the high frequency gain. Both n_p and n_u control the roll-off rates of the filters, equal to 1 in this case i.e. first order filters. The controller output is fixed, as this is only the applied voltage to the EMS system. The controller inputs, however, vary based upon the utilised sensor set. i.e., Single-Input-Single-Output controller for 1 sensor; Multiple-Input-Single-Output controllers for more sensor combinations. Moreover, the order of the controller is fixed to the order of the plant plus the order of the chosen filters i.e. $3 + 2 = 5^{th}$ order controller. Although the order of the controller is low if higher order controllers are necessary then controller reduction techniques can be easily adopted to the proposed framework as shown in [17].

3) Multiobjective \mathcal{H}_∞ LSDP control for the EMS: The design of the controller is based on the normalised coprime-factor plant description, proposed by [18], which incorporates the simple performance - robustness trade-off obtained in loop shaping, with the normalised Left Coprime Factorization (LCF) robust stabilization method as a means of guaranteeing closed-loop stability. The design method proceeds by shaping the open-loop characteristics of the plant using the weighting functions W_1 and W_2 . The plant is temporarily redefined as $\hat{G}(s) = W_2 G W_1$ and the \mathcal{H}_∞ controller $\hat{K}(s)$ is calculated. In the final stage, the weighting functions are merged with the controller by defining the overall controller $K(s) = W_1 \hat{K} W_2$. The size of model uncertainty is quantified by the stability radius ϵ , i.e. the stability margin. For values of $\epsilon \geq 0.25$, 25% coprime factor uncertainty is allowable. However, in this paper a relaxed constraint is used to have $\epsilon \geq 0.15$ instead (refer to [2] for more details). A typical approach would aim to keep the filters and thus controller as simple as possible. Thus, the W_1 pre-compensator, is chosen as a single scalar weighting function set to unity. For the W_2 post-compensators there can be five weighting functions that are used depending on the selected sensor set. The airgap, $(z_t - z)$, measurement is a compulsory measurement required for proper maglev control of the magnet distance from the rail and thus a low pass filter ($W_{(z_t - z)} = W_p$) is chosen with integral action allowing zero steady state airgap error (for the nominal performance). The weighting functions are given as $W_1 = 1$ and $W_2 = \text{diag}(W_i, W_b, W_{(z_t - z)}, W_{\dot{z}}, W_{\ddot{z}})$.

B. Sensor Fault Tolerance Scheme

Fault tolerance is a subject that has been a main point of research in the last years [3]. In this paper the aim is to recover the stability and performance under multiple sensor failures. In this context, the Active Fault Tolerant Control

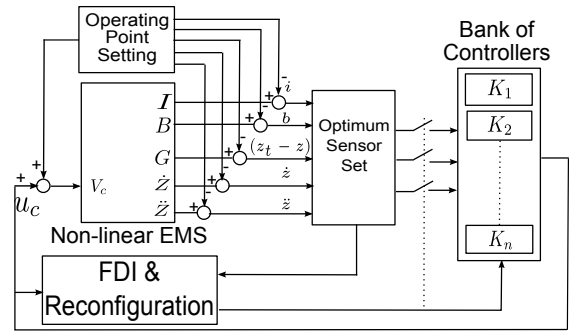


Fig. 3. AFTC diagram for multiple sensor failures.

(AFTC) concept is used. The AFTC concept is composed from a Fault Detection and Isolation (FDI) mechanism and a bank of pre-designed controllers. When multiple sensor faults happen remedial actions are taken by controller re-configuration. The recovery of the performance is aimed by using the remaining healthy sensors (sub-set of the selected sensor set) as depicted in Fig. 3. An FDI mechanism is included in order to detect and isolate the faulty sensors and

produce the controller reconfiguration signal. It is assumed that the switching is fast enough not to affect stability or cause large delays in the system. Typically, a common way to detect a fault is to monitor the residual of two signals. The residuals for each output is typically produced by means of dedicated observers. A bank of dedicated observers (i.e. $K_{o_1}, K_{o_2}, \dots, K_{o_n}$) is used to monitor the condition of each sensor as depicted in Fig. 3. Isolating the faulty sensors is done by taking the sensor out of the loop in such a way that the faulty signal is not fed to the new controller (i.e. switching). Sensor faults modelling can be done in three ways: abrupt fault, incipient fault and intermittent fault.

V. RESULTS

Simulations were performed in MATLAB without Java functions. This helps reducing the necessary computational power for the completion of the algorithm. The computer used is a typical PC with 2.93GHz clock speed. The controller selection criteria f_{c_i} and f_k in each control method are listed in Table III.

The controller selection criteria are set as follows:

- 1) LQG: The controller selection criteria aim to select a controller that results to the best ride quality and an input current of $2A_{rms}$.
- 2) $\mathcal{M.O.} \mathcal{H}_\infty$: The controller selection criteria, seeks for controller that results to a reasonable ride quality with a noise level less than $10V_{rms}$ and maximized robustness margin.
- 3) \mathcal{H}_∞ LSDP: The controller with reasonable ride quality, the minimum noise level and maximum robustness margin is aimed to be selected.

TABLE III
OBJECTIVE FUNCTIONS FOR EACH CONTROL METHOD

	LQG	$\mathcal{M.O.} \mathcal{H}_\infty$	\mathcal{H}_∞ LSDP
f_{c_1}	$\ddot{z}_{rms} \leq 0.5m/s^2$	$\ddot{z}_{rms} \leq 0.5m/s^2$	$\ddot{z}_{rms} \leq 0.5m/s^2$
f_{c_2}	$i_{rms} \leq 2A$	$u_{c_{rms}} \leq 10V$	$u_{c_{rms}} \leq 10V$
f_k	$min(\ddot{z}_{rms})$	$min(\gamma)$	$max(\epsilon)$

Given that the optimisation of the control system is done via GAs the framework requires significant computational power, which depends on issues such as the number of constraints required, the control design method, the number of variables and the heuristic type of optimisation. In Table V the time taken for the completion of the algorithm, t_t , is given with a typical PC. In terms of notation, t_t is the total time required for the optimisation of each sensor set for the EMS system having a total of N_s sensor sets. The largest t_t is 152 hours for the $\mathcal{M.O.} \mathcal{H}_\infty$ and for the other two controller design methods 54 and 45. However, note that the \mathcal{H}_∞ LSDP total number of sensor sets is 16 while for the other two methods 31. Therefore, it can be concluded that the LQG method requires less computational power. Additionally, the framework was able to identify the total number of sensors that satisfy Ω , $N_{y_{\Omega=0}}$ for each control method. There are 24 for the LQG, 20 for the $\mathcal{M.O.} \mathcal{H}_\infty$ and 11 for the \mathcal{H}_∞ LSDP. This is another interesting point, i.e.

the LQG method needs less computational effort and gives the higher number of sensor sets that satisfy Ω , i.e. $N_{y_{\Omega=0}}$. Some of the results obtained from the framework are listed

TABLE V
COMPARISON FOR EACH CONTROL METHOD.

	LQG	$\mathcal{M.O.} \mathcal{H}_\infty$	\mathcal{H}_∞ LSDP
N_s	31	31	16
$N_{y_{\Omega=0}}$	24	20	11
t_t (hrs)	54	150	45

on Table IV. The corresponding columns list the Ω and SFAR values for each controller design method. The Ω is marked, \checkmark , if the control constraints are satisfied otherwise is marked 'x'. As for the \mathcal{H}_∞ LSDP controller design the airgap is a standard measurement, symbol '*' indicates the sensor sets that do not include the airgap measurement and hence not optimised. Moreover, the framework aim to find *stable* and stabilising controllers, hence '-' indicates cases where no stable controller could be found. Additionally, the SFAR is given a value of zero in two cases: (i) Ω is not satisfied and/or (ii) the sensor set contains only one sensor. Referring to the Ω columns, the first point one can notice is that the performance of the EMS system not significantly changed remains unchangeable even if more sensors are added in the loop e.g. $id_{LQG} : 1$ has one sensor while $id_{LQG} : 15$ has 5 sensors. It is also worth mentioning that adding more sensors could actually degrade the performance of the system e.g. refer to $id_{LSDP} : 10$.

1) *Optimised sensor selection for control*: If one needs to consider only the control of the EMS system the LQG control method is the only that works satisfactorily with single measurements. On one hand the $\mathcal{M.O.} \mathcal{H}_\infty$ does not give sufficient performance with single measurements and on the other hand the \mathcal{H}_∞ LSDP only the id:2 satisfy Ω but not the f_{c_i} . however it could be used for fault tolerance purposes. In conclusion the sensor sets with $id_{LQG} : 1$ or 3 results to adequate performance of the EMS system.

2) *Optimised sensor selection for fault-tolerant control*: Looking the simulation results from the optimised sensor selection for FTC, the SFAR metric is introduced to simplify the selection. The SFAR as explained in Section II indicates the capacity of the sensor set to offer fallback options. The SFAR values are varied between 28% and 100%. The highest values of the SFAR are evaluated for the $id_{LQG} : 6$, and $id_{\mathcal{H}_\infty LSDP} : 4, 7$. The SFAR is evaluated with different values independent from the number of the sensor sets and the following points are emphasised:

- For the $id : 4$ $SFAR_{LQG}=50\%$, $SFAR_{\mathcal{M.O.} \mathcal{H}_\infty} = 0\%$ and $SFAR_{\mathcal{H}_\infty LSDP} = 100\%$
- For the $id : 6$ the SFAR with LQG is 100% but for the other control methods zero.
- For the $id : 7$ the $SFAR_{\mathcal{H}_\infty LSDP} = 100\%$ but for the other two control methods zero. Note that f_{c_i} is not satisfied.
- for the $id : 8$ the SFAR is given as 83%, 28% and is not evaluated for the LSDP method because it does not

TABLE IV
COMPARISON OF THE PROPOSED FRAMEWORK USING VARIOUS MODERN CONTROL METHODS.

id	Sensor Set	LQG		$\Omega_{\mathcal{H}_\infty}$	$\mathcal{M.O.H}_\infty$			Ω_{LSDP}	\mathcal{H}_∞ LSDP		
		Ω_{LQG}	SFAR _{LQG}		f_{c_i}	f_k	SFAR _{\mathcal{H}_∞}		f_{c_i}	f_k	SFAR _{LSDP}
1	b	✓	0	-	-	-	-	*	*	*	*
2	$(z_t - z)$	x	0	x	x	x	0	✓	x	✓	0
3	\dot{z}	x	0	-	-	-	-	*	*	*	*
4	\ddot{z}	✓	0	-	-	-	-	*	*	*	*
5	$b, (z_t - z)$	✓	50	✓	x	✓	0	✓	✓	✓	100
6	b, \ddot{z}	✓	100	-	-	-	-	*	*	*	*
7	$(z_t - z), \dot{z}$	x	0	✓	✓	✓	0	✓	x	✓	100
8	i, b, \ddot{z}	✓	83	✓	✓	✓	28	*	*	*	*
9	$i, (z_t - z), \ddot{z}$	✓	50	✓	x	✓	28	✓	✓	✓	33
10	$b, (z_t - z), \ddot{z}$	✓	83	✓	✓	✓	28	x	x	x	0
11	$i, b, (z_t - z), \dot{z}$	✓	42	✓	✓	✓	46	✓	✓	✓	71
12	$i, (z_t - z), \dot{z}, \ddot{z}$	✓	50	✓	✓	✓	53	✓	✓	✓	71
13	$i, b, (z_t - z), \dot{z}, \ddot{z}$	✓	73	✓	✓	✓	61	✓	✓	✓	66

includes the airgap sensor.

- Looking at sensor set $id : 10$ the SFAR for the LQG and the \mathcal{H}_∞ are 83% and 28% respectively but for the other control method is zero as the SFAR is not evaluated.
- The SFAR values for the LQG, the $\mathcal{M.O.H}_\infty$ and the \mathcal{H}_∞ are similar 73%, 61% and 66%.

With respect to the above considerations in mind the two sensor sets that give optimised performance with the highest SFAR are the $id_{\mathcal{H}_\infty LSDP} : 4$ and $id_{LQG} : 6$. Hence, the practical engineer could consider the above two sets of sensor configuration as a starting point providing a good level of control and fault tolerance. Finally, reliability of the proposed sensor selection method can be tested using the proposed AFTC method presented in Section IV-B. Results for the tests of the three MCM are presented and analysed in [10], [11] and [12].

VI. CONCLUSIONS

A comparison between three different MCM in the context of the proposed sensor optimisation framework is presented in this paper. The framework is applied to an EMS system and the results show that the framework is capable of identifying sensor sets that could be used to control the EMS ensuring properties like optimised performance, robustness and reliability of such safety-critical system. The proposed scheme aims to alleviate complexity in the design for control and fault tolerance. With increasing complexity of the system under consideration and the required constraints in the design, computational power requirements in finding the solution may be a drawback. However, the procedure is an off-line process and attempts to introduce a level of simplification in the choice of the sensor sets for the practical engineer.

REFERENCES

- [1] M. V. De Wal and B. De Jager. A review of methods for input/output selection. *Automatica*, 37(4):487–510, 2001.
- [2] S. Skogestad and I. Postlethwaite. *Multivariable Feedback Control Analysis and Design*. John Wiley & Sons Ltd, 2nd Edition, New York, 2005.
- [3] Inseok Hwang, Sungwan Kim, Youdan Kim, and Chze Eng Seah. A survey of fault detection, isolation, and reconfiguration methods. *IEEE Transactions on Control Systems Technology*, 18(3):636–653, 2010.
- [4] Aimin Zhou, Bo-Yang Qu, Hui Li, Shi-Zheng Zhao, Ponnuthurai Nagarathnam Suganthan, and Qingfu Zhangd. Multiobjective evolutionary algorithms: A survey of the state of the art. *Swarm and Evolutionary Computation*, 1(1):32–49, 2011.
- [5] J. Dreoo, P. Siarry, A. Petrowski, and E. Taillard. *Metaheuristics for Hard Optimization*. Springer-Verlg Berlin Heidelberg, New York, 2006.
- [6] Abdullah Konak, David W. Coit, and Alice E. Smith. Multi-objective optimization using genetic algorithms: A tutorial. *Reliability Engineering and System Safety*, 91(9):992–1007, 2006.
- [7] P. J. Fleming and R. C. Purshouse. Evolutionary algorithms in control systems engineering: A survey. *Control Engineering Practice*, 10(11):1223–1241, 2002.
- [8] Kalyanmoy Deb, Amrit Pratap, Sameer Agarwal, and T. Meyarivan. A fast and elitist multiobjective genetic algorithm: Nsga-ii. *IEEE Transactions on Evolutionary Computation*, 6(2):182–197, 2002.
- [9] C. A. C. Coello. Theoretical and numerical constraint-handling techniques used with evolutionary algorithms: A survey of the art. *Computer Methods in Applied Mechanics and Engineering*, 191(11-12):1245–1287, 2002.
- [10] K. Michail, A. Zolotas, and M. R. Goodall. Optimised configuration of sensors for fault tolerant control of an electromagnetic suspension system. *International Journal of Systems Science*, 43(10):1785–1804, 2012.
- [11] K. Michail, A. Zolotas, and R. Goodall. An optimum sensor selection design framework applied to an electro-magnetic suspension system. In *1st Conference on Control and Fault-Tolerant Systems*, pages 684–689, 2010.
- [12] K. Michail, C. A. Zolotas, M. R. Goodall, and G. Halikias. Optimal selection for sensor fault tolerant control of an ems system via loop-shaping robust control. In *19th Mediterranean Conference on Control and Automation*, pages 1112–1117, 2011.
- [13] R. M. Goodall. Generalised design models for ems maglev. In *Proceedings of MAGLEV 2008 - The 20th International Conference on Magnetically Levitated Systems and Linear Drives*, 2008.
- [14] K. Michail. Optimised configuration of sensing elements for control and fault tolerance applied to an electro-magnetic suspension system, PhD dissertation, Loughborough University, Department of Electronic, Electrical and Systems Engineering, 2009. <http://hdl.handle.net/2134/5806>.
- [15] R. M. Goodall. The theory of electromagnetic levitation. *Physics in Technology*, 16(5):207–213, 1985.
- [16] R. M. Goodall. Dynamics and control requirements for ems maglev suspensions. In *Proceedings on international conference on Maglev*, pages 926–934, 2004.
- [17] K. Michail, Y. Zhou, A. Zolotas, R. Goodall, and G. Halikias. Optimised sensor configurations with reduced order controllers applied to an ems system. In *29th Chinese Control Conference*, pages 3595–3600, 2010.
- [18] D. C. McFarlane and K. Glover. A loop-shaping design procedure using H_∞ synthesis. *IEEE Transactions on Automatic Control*, 37(6):759–769, 1992.